Available online at www.sciencedirect.com
ScienceDirect
Energy Conversion and Management 48 (2007) 528–538
ENERGY CONVERSION & MANAGEMENT
www.elsevier.com/locate/enconman

Theoretical and experimental study of a small unit for solar desalination using flashing process

A. Safwat Nafey [a,*], M.A. Mohamad [b], S.O. El-Helaby [a], M.A. Sharaf [a]

[a] Department of Engineering Science, Faculty of Petroleum and Mining Engineering, Suez Canal University, Suez 43522, Egypt
[b] Solar Energy Department, National Research Center, Cairo, Egypt

Received 3 December 2005; accepted 15 June 2006
Available online 1 September 2006

Abstract

A small unit for water desalination by solar energy and a flash evaporation process is investigated. The system is built at the Faculty of Petroleum and Mining Engineering at Suez, Egypt. The system consists of a solar water heater (flat plate solar collector) working as a brine heater and a vertical flash unit that is attached with a condenser/preheater unit. In this work, the system is investigated theoretically and experimentally at different real environmental conditions along Julian days of one year (2005). A mathematical model is developed to calculate the productivity of the system under different operating conditions. The BIRD's model for the calculation of solar insolation is used to predict the solar insolation instantaneously. Also, the solar insolation is measured by a highly sensitive digital pyranometer. Comparison between the theoretical and experimental results is performed. The average accumulative productivity of the system in November, December and January ranged between 1.04 to 1.45 kg/day/m^2. The average summer productivity ranged between 5.44 to 7 kg/day/m^2 in July and August and 4.2 to 5 kg/day/m^2 in June.

Keywords: Desalination; Flash unit; Solar water heater; Solar energy

1. Introduction

Global resources of fresh water are scarce, unevenly distributed and, in many cases, may require some form of treatment and handling. These limited resources have resulted in water shortages in 88 developing countries across the world containing 50% of the world's population [1]. The need for purification of saline water is increasing due to an increase of population and the limited supply of potable water. Using solar energy is a practical method for obtaining small amounts of fresh water from saline water. Solar water distillation has been a subject of great interest for several decades [2]. The standard techniques like multi-stage flash, multi-effect distillation, vapor compression and reverse osmosis are reliable for large capacity ranges of (100–50,000) m^3/day of fresh water production.

However, these technologies are expensive for small amounts of fresh water. Moreover, they can not be used in locations where there are limited maintenance facilities. In addition, the use of conventional energy sources to drive these technologies has a negative impact on the environment [3]. Solar desalination techniques are considered to be clean operations for producing clean water from saline water. Also, the techniques of solar desalination are many and vary according to the size of the demand for fresh water and the size of solar energy present. El-Nashar presents a small solar multi-effect distillation (MED) unit for seawater desalination processes for remote arid areas [4]. A solar stand alone system consisting of a multi-effect stack (MES) evaporator supplied by thermal energy from flat plate or evacuated tube collectors with pumping power supplied by a solar PV system was investigated [5]. Lourdes Garcia-Rodriguez presented a preliminary design for different solar systems of seawater distillation processes. The solar collectors were parabolic troughs in which brine

* Corresponding author. Tel.: +20 62 3303560; fax: +20 62 3366252.
E-mail address: swazy20@hotmail.com (A.S. Nafey).

0196-8904/$ - see front matter © 2006 Published by Elsevier Ltd.
doi:10.1016/j.enconman.2006.06.010

Nomenclature

A	Area in m^2, or a parameter used in Eq. (21)
A_1	Condenser heat transfer area (m^2)
A_c	Collector heat transfer area (m^2)
A_e	Collector effective area (m^2)
A_p	Collector absorber area (m^2)
B	Brine, or a parameter used in Eqs. (21) and (22)
B_o	Mass flow rate of the brine entering the flash unit (kg/s)
B_1	Mass flow rate of the brine exiting from the 1st flash unit (kg/s)
BPR	Boiling point elevation of saline water parameter
b	The thickness of the bond (m)
C	Parameter used in Eqs. (21) and (22) or the collector heat capacity
C_p	Bond conductance
C_h	Collector height (m)
C_L	Collector length (m)
C_W	Collector width (m)
c_p	Specific heat capacity of saline water (kJ/kg K)
D	Distillate or parameter used in Eq. (21)
DP	Distillate product kg/h
D_1	Distillate product from the 1st stage (kg/s)
d	Collector tube outer diameter (m)
E	Parameter used in Eq. (20)
F	Fin efficiency
$F_{i,o}$	Inlet and outlet feed water to the condenser (kg/s)
FPC	Flat plate collector
FF	Flooding factor
F'	Efficiency factor for solar collector
F_R	Heat removal factor
F_S	Feed water system (kg/s)
G	Parameter by Eq. (10) ($kg/s/m^2$)
H_{v1}	Latent heat of vaporization of water (kJ/kg)
h_f	Fluid heat transfer coefficient (W/m^2 K)
h_o	Enthalpy stream of the inlet brine to the stage (W/m^2 K)
h_{b1}	Enthalpy stream of the outlet brine from the stage (kJ/kg)
h_{D1}	Enthalpy stream of the distillate product (kJ/kg)
$h_{Fi,o}$	Enthalpy stream of the inlet and outlet feed water to the condenser (kJ/kg)
h_w	Convection heat transfer coefficient (W/m^2 K)
I_S	Solar intensity (W/m^2)
ID_1	Inner diameter of the condenser tubes (m^2)
k_b	Back insolation conductivity (W/m K)
k_e	Edge insolation conductivity (W/m K)
k	Thermal conductivity (W/m K)
l	Length (m)
l_b	Back insolation thickness (m)
l_e	Edge insolation thickness (m)
$m_{Fi,o}$	Mass flow rate of feed water in and out of the condenser (kg/s)
NEA	Non equilibrium allowance
NG	No. of glass covers of the collector
NTU_1	No. of transfer unit parameter for the flash unit
OD_o	Outer diameter of the condenser tubes (m^2)
P	Pressure (kPa)
PR	Unit performance ratio
P_{d1}	Vacuum pressure at distillate outlet port (kPa)
Q_1	Thermal energy of the condenser in steady state (W)
Q_u	Useful energy from the collector (W)
Q_{loss}	Energy loss from the collector (W)
Q_{stg}	Energy stored in the collector (W)
R_F	Stage fouling factor
S_t	Tube spacing (m)
TBT	Top brine temperature (°C)
T_{amb}	Ambient temperature (°C)
T_{bo}	Inlet brine stream temperature to the flash stage (°C)
T_{b1}	Outlet brine stream temperature from the flash stage (°C)
$T_{i,ocol}$	Inlet and outlet brine stream temperature to the collector (°C)
T_{d1}	Distillate product stream temperature (°C)
$\bar{T}_f$	The fluid temperature through the collector (°C)
$T_{Fi,o}$	Inlet and outlet feed temperature of the condenser (°C)
T_g	Collector glass cover temperature (°C)
T_{ins}	Collector insulation temperature (°C)
ΔT_{lm1}	Logarithmic mean temperature (°C)
T_{mp}	Mean plate temperature of the collector (°C)
T_p	Plate temperature of the collector (°C)
T_{v1}	Vapor temperature (°C)
U_b	The bottom loss coefficient (W/m^2 K)
U_e	The edge loss coefficient (W/m^2 K)
U_1	Overall heat loss of the stage (W/m^2 K)
U_t	Overall top loss in the collector (W/m^2 K)
U_l	Overall losses in the collector (W/m^2 K)
V_w	Wind speed (m/s)
x_f	The salinity of inlet feed water (ppm)
$x_{bo,1}$	Salt concentration for both streams inlet hot feed and wasted brine (ppm)
η_c	Collector intravenous thermal efficiency
β	Collector tilt angle
σ	Boltzmann constant
ε_g	Emittance of glass cover
ε_p	Emittance of absorber plate
δ	Fin thickness (m)
$\tau\alpha$	Transmittance-absorptance product
ϕ	Tube side brine velocity (m/s)

circulated as the thermal fluid. Steam is directly obtained from the circulating brine. The solar collector field could be connected to condenser/preheater heat exchangers; but nevertheless, the system would have a low performance ratio. Badran et al. [6] presented a flat plate solar collector coupled with solar still unit. The experimental investigation was made to study the effect of coupling a flat plate solar collector on the productivity of solar stills. It has been found that coupling of a solar collector with a still has increased the productivity by 36%. The still area was about 1 m^2 filled with brackish water supplied to it from a collector. The flat plate collector area was found to be about 1.08 m^2. The system total productivity was found to give 3.51 kg/day and found to be 36% more than that when the still was operated alone (2.24 kg/day). Also Soliman et al. [3] examined a humidification dehumidification desalination system powered by solar concentrator collector (area = 2.5 m^2) with total unit productivity equal to 8 kg/day. Multi-stage flash desalination (MSF) is currently the workhorse of the desalination industry with a market share close to 60% of the total world production capacity [1]. Actually, a small range of top brine temperature beginning from 50 °C can operate MSF processes. Solar stills, solar ponds and solar collectors can produce these small ranges of temperatures needed in flashing process. Kriesi [7] constructed a conventional 6 m^3/day MSF plant with a brine maximum temperature of 120 °C and coupled with a concentrating solar greenhouse collector and a hot water storage tank. Also scheme for large-scale desalination of seawater by solar energy and MSF process was manufactured in Thar desert of India [8]. The scheme was designed to produce about 5.25×10^7 m^3/year of fresh water with 11.52 km^2 of collector area. Ziad et al. [9] presented a single flash unit powered by a flat plate solar collector. The maximum allowable top brine temperature was ranged between 50–70 °C. However, the process is still in needs for more theoretical and experimental investigation. In the present work (a small size flash unit) is powered with solar energy for producing a small amount of potable water. This system is designed and tested at the Faculty of Petroleum and Mining Engineering at Suez-Egypt. The system is mainly consists of a flat plate solar collector (FPC) with total surface area about 2.39 m^2, and a flash evaporation unit. The system is operated and investigated outdoor during winter and summer seasons. Generally, the total productivity of the system in winter ranged between 1.04 to 1.45 kg/day/m^2, and the summer productivity ranged between 4.2 to 7 kg/day/m^2. The main objective of this study is to perform a theoretical and experimental investigation of the process performance under real operating conditions. Also the effect of different operating conditions is investigated and presented.

2. System description and experimental work procedure

Fig. 1 shows the system components. Simply, the system containing the solar water heater (FPC) (1) and flash

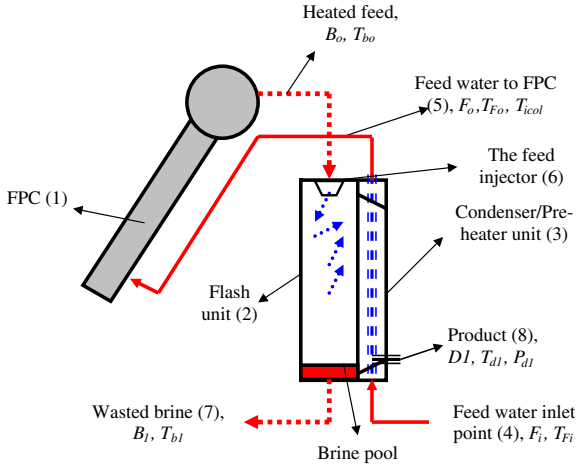

Fig. 1. A schematic diagram of the test rig.

evaporation unit (2) is designed vertically and attached to the condenser/preheater unit (3). Feed water enters the condenser inlet point (4) at a known temperature then passing through the condenser (5) with a higher temperature value caused by the heat transferred from the vapor that condensates across the outside surface of the condenser tubes. Then, the feed water enters the solar collector with its new (higher) temperature to raise it to the top brine temperature (TBT) before entering the flash chamber. Then, the hot feed water enters the flash chamber by passing through the brine injector (6). The feed water injector is operated at maximum flow rate equal to 0.05 kg/s and minimum flow rate equal to 0.013 kg/s. On the other hand, the wasted brine (7) then exit after releasing its vapor.

2.1. Flash evaporation unit

The flash chamber is designed as a steel cylindrical chamber coated with epoxy steel to prevent outside environmental corrosion effects and to reduce the thermal losses to the ambient. The height of the flash chamber is 1 m with a diameter of 0.5 m. The brine depth should be kept as low as possible to avoid high non-equilibrium losses, brine entrainment, and stage flooding [16]. The brine level is controlled to be not exceeding about 0.2 m in the flash chamber. Fig. 2 shows the flash unit attached to the condenser unit. Fig. 3 shows a photograph of the flash chamber without being attached to the condenser unit.

The hot feed water enters the flash chamber through the feed water injector at a pressure equal to 2.5 bar when operating at maximum flow rate, and 1.5 bar when operating at minimum flow rate. The injector is designed to control the feed water to the system by a control valve has a three opening positions.

2.2. The condenser/preheater unit

The main parts of condenser unit are copper tubes, upper and lower headers and the outside cover. The tubes

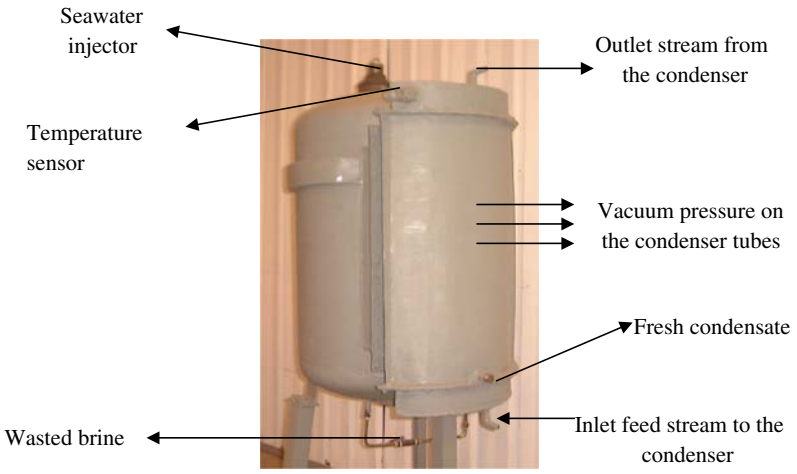

Fig. 2. The photograph of the flash chamber attached to the condenser unit.

across the condenser unit are made from copper with thermal conductivity 387 W/mK. The tube length is 0.65 m and the inner diameter is 0.008 m and the outer diameter is 0.0098 m. The number of tubes is 69 tubes to perform a total length of about 45 m and total condenser area equal to 1.388 m^2. Every tube bank contains 5 tubes staggered distribution. The tubes are welded at their ends by an epoxy steel welding material in a flange made of steel copper to prevent leakages. To fix the condenser to the flash unit without any leakages; a rubber frame is welded to the condenser. Fig. 4 shows a photograph of the condenser at different views with its inside tubes without covering or headers.

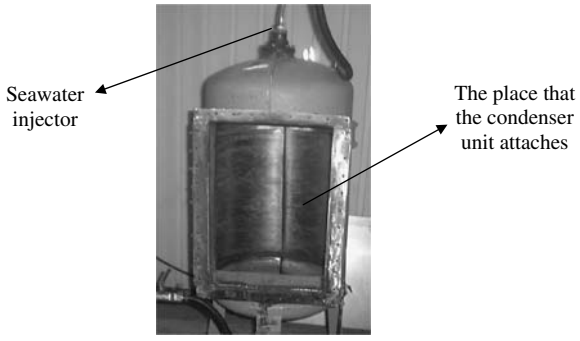

Fig. 3. The flash chamber without its condenser.

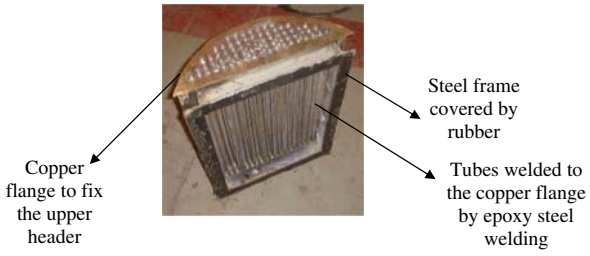

Fig. 4. View of the condenser unit with its tubes.

Table 1
The manufactured characteristics of the collector

Absorber material	Aluminum plate thickness = 0.5 mm
Collector area	$A_c = 2.39$ m^2
Absorber area	$A_p = 2.1$ m^2
Effective area	A_e = 88% of the collector area
Coating absorptance	92%
Coating emittance	15%
Glass cover transmittance	91%
Insulation thickness	37 mm
Absorber thickness	Aluminum steel = 0.5 mm
Glass cover thickness	3 mm
Collector weight	58.5 kg
Tube risers mean diameter	16 mm
Tube headers mean diameters	28 mm
Tube spacing across the collector	$S_t = 16.3$ cm
Risers tube length	1.81 m
The plate to glass cover spacing	70 mm
Number of glass cover	1

Where A_c is the collector total area, A_p is the plate heat transfer area, A_e is the collector effective area, S_t is the tube spacing.

2.3. Solar collector (feed water heater)

The feed water heater in this work is a flat plate solar collector. The collector is manufactured by Solar Energy Corporation Foundation at Cairo, Egypt. The collector technical data are listed in Table 1.

The collector is operated with a slope angle of 45°. The collector aspect degree is 180° south. The connections tubes between the collector and the flashing unit are made of plastic material and insulated by reflectance material. The tubes are made of plastic to reduce thermal losses to the ambient. The diameter of the plastic tubes is 3/4 inch. The position of the collector is 3 m above the flashing unit.

3. Measurements of experimental data

3.1. Temperature

The different temperatures of the system (see Fig. 1) are measured by a digital volt meter through signals provided

by the thermocouples located at the measurement points, which have been demarcated and have the accuracy of ±0.1 °C. The range of operation of the voltmeter is 10 mV and the relative error is less than 1%. The ambient temperature is measured with a common glass-tube-mercury temperature meter. The proper error of the temperature meter is less than 0.5 °C.

3.2. Solar radiation and wind velocity

Solar radiation is measured by a solar radiation pyranometer laid on the collector surface with slope angle equal to 45°. The error of the device is about ±3%. An anemometer is used to measure the wind speed in m/s.

3.3. Pressure

The inlet feed water and vacuum pressures are measured by pressure sensors. The pressure sensor for the inlet feed water is put directly after the brine injector valve. The vacuum pressure sensor is put at the distillate outlet valve.

3.4. Condensate and wasted brine flow rates

By collecting the condensate and outlet wasted brine in two calibrated tanks at a certain time, the flow rate of both the condensate and brine can be measured.

4. Mathematical model

The process mathematical model consists of two parts. The first part is for estimating the solar intensity. To estimate the solar radiation at the location of operation, Bird's model [10] is employed. The model is constructed from some correlations (atmospheric conditions, ozone absorptance, ozone scattering, water vapor column, ground and sky's albedos...) that give its results based on knowing some initial data (Julian day, solar angles...). A computer program is developed to evaluate this model. The model gives the more matched results with the measured data for Suez-Gulf area. The second part containing the equations representing the process units. Using the measured values of solar intensity, wind velocity, ambient temperature and all operating parameters (temperatures and pressures), the daily productivity of the system can be calculated by the developed program. The energy balance equations of the test rig could be written and presented as follows with the following assumptions:

1. The fluid used in all experiments is water.
2. Thermal losses to the ambient are neglected.
3. Feed water flow rate considered constant along the operation day.
4. The energy stored in the collector is neglected.
5. The accumulative vapor temperature T_{d1} is nearly the same as the outlet fluid temperature T_{Fo} from the condenser.

The system goes under steady state condition.

4.1. Mathematical model for the flat plate solar collector

The energy balance equation of the solar collector can be written as follows [12]:

$$I_S \times A_c = Q_{loss} + Q_u + Q_{stg} \tag{1}$$

where I_S is the energy from the sun, and estimated by BIRD's model [10]. A_c is the collector surface area, Q_{loss} is the heat loss from the collector and Q_u is the useful energy transferred from the absorber to the flash chamber. Q_{stg} is the energy stored in the collector and is neglected. The heat loss is expressed by Frederick [12] as

$$Q_{loss} = A_c U_l F'(\bar{T}_f - T_{amb}) \tag{2}$$

$\bar{T}_f$ is the average fluid temperature through the collector.

The overall heat transfer coefficient of the collector U_l is the summation of three components; the top loss U_t, the bottom loss U_b, and the edge loss U_e and the other variables are defined in the nomenclature.

$$U_l = U_t + U_b + U_e \tag{3}$$

where the bottom and edge losses are calculated respectively as following [15]:

$$U_b = k_b/l_b \tag{4}$$

$$U_e = (k_e/l_e) \times \frac{2(C_L + C_W)C_h}{C_L \times C_W} \tag{5}$$

An empirical equation for the top losses U_t for both hand and computer calculations was developed by Klein (1975) [13].

$$U_t = \left[\frac{NG}{\frac{C}{T_{mp}}\left[\frac{(T_{mp}-T_{amb})}{(NG+f)}\right]^e} + \frac{1}{h_w}\right]^{-1} + \frac{\sigma(T_{mp}+T_{amb})(T_{mp}^2+T_{amb}^2)}{(\varepsilon_p + 0.00591NG \times h_w)^{-1} + \frac{2NG+f-1+0.133\times\varepsilon_p}{\varepsilon_g} - NG} \tag{6}$$

where NG is the number of glass covers, $f = (1 + 0.089h_w - 0.1166h_w\varepsilon_p)(1 + 0.07866NG)$, $C = 520 \times (1 - 0.000051\beta^2)$ for $0° < \beta < 70°$, $e = 0.43(1 - 100/T_{mp})$, where β is the collector tilt angle in degree and h_w is the wind heat transfer coefficient and given by [11] as

$$h_w = 5.7 + 3.8 \times V_w \tag{7}$$

After evaluating the overall top loss U_t, the efficiency factorF' of Eq. (2) can be calculated as follows:

$$F' = \frac{\frac{1}{U_t}}{s\left(\frac{1}{U_t[(s_t-d)F+d]} + \frac{1}{\frac{h_f}{7}} + \frac{1}{h_f \pi d_i}\right)} \tag{8}$$

where the collector fin efficiency F is given by [11]

$$F = \frac{\tanh\left[\sqrt{\frac{U_t}{k\delta}\left(\frac{s_t-d}{2}\right)}\right]}{\sqrt{\frac{U_t}{k\delta}\left(\frac{s_t-d}{2}\right)}} \quad (9)$$

Also the heat removal factor is calculated from [11]

$$F_R = F' \times \frac{GC_p}{U_l F'}\left(1 - \exp - \left(\frac{U_t F'}{GC_p}\right)\right) \quad (10)$$

where $G = m/A_c$. Once F_R is calculated, the useful energy from the collector can be calculated from the following equation:

$$Q_u = F_R A_c[I_s - U_l(T_{icol} - T_{amb})] \quad (11)$$

4.2. Mathematical model for the flashing unit

For this part, the mathematical model is based on the following assumptions:

1. The distillate product is salt free.
2. The flash chamber is in equilibrium with the brine leaving the stage.
3. The distillate vapor always condenses completely.
4. The flow of noncondensables is negligible.

The energy balance for the flashing brine (see Fig. 5) is expressed as follows:

$$\dot{B}_o h_o(T_{bo}, x_{bo}) = \dot{B}_l h_{bl}(T_{bl}, x_{bl}) + [(\dot{B}_o - \dot{B}_l) H_{Vl}(T_{bl}, P(T_{bo}))] \quad (12)$$

where Eqs. (13) and (14) below shows the overall mass balance for both flash and condenser units

$$\dot{B}_o = \dot{D}_l + \dot{B}_l \quad (13)$$

$$\dot{F}_i = \dot{F}_o \quad (14)$$

And the flash unit enthalpy balance is

$$\dot{B}_o h_o + \dot{F}_i h_{Fi} = \dot{B}_l h_{bl} + \dot{D}_l h_{dl} + \dot{F}_o h_{Fo} + Q_{loss} \quad (15)$$

while the overall heat transfer coefficient is represented by the following equation [14]:

$$U_l = f(\phi, T_{Fi}, T_{Fo}, T_{Dl}, ID_l, OD_o, FF, R_F) \quad (16)$$

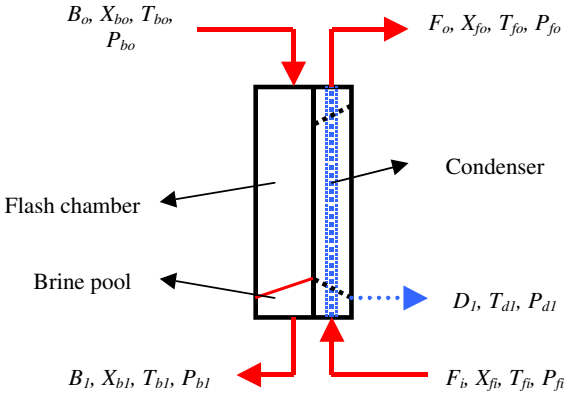

Fig. 5. A flash stage unit.

The amount of heat exchanges across the condenser heat transfer surface Q_l is calculated by Eq. (17),

$$Q_l = \dot{m}_{Fi,o} c_p (T_{Fo} - T_{Fi}) = U_l A_l \times \Delta T_{lml} \quad (17)$$

From Eq. (17),

$$\frac{U_l \times A_l}{\dot{m}_{Fi,o} c_p} = \ln\frac{T_{dl} - T_{Fi}}{T_{dl} - T_{F0}} = -\ln\frac{T_{dl} - T_{F0}}{T_{dl} - T_{Fi}} \quad (18)$$

From Eq. (18), and after a few steps of simplification; the following equation is obtained:

$$(1 - E) \times T_{Fi} + E \times T_{dl} - T_{Fo} = 0 \quad (19)$$

where $E = 1 - e^{-NTU_l}$ and $NTU_l = U_l \times A_l / \dot{m}_{Fi,o} c_p$

For the equilibrium correlation; the relation between the outlet brine temperature T_{bl} and the distillate vapor temperature T_{dl} is presented by Eq. (20):

$$T_{dl} = T_{bl} - NEA - BPR \quad (20)$$

The non-equilibrium allowance NEA and BPR are calculated by the following equations [14]; where

$$NEA = A + B \times T_{bl} + C \times T_{bl}^2 + D \times T_{bl}^3 \quad (21)$$

where $A = 2.556$, $B = -0.203E{-}1$, $C = -0.129E{-}1$, and $D = 0.1123E{-}5$

$$BPR = (B + C \times x_f) \times x_f \quad (22)$$

where

$$10^3 \times B = 6.71 + 6.43 \times 10^{-2} \times T_{bl} + 9.74 \times 10^{-5} \times T_{bl}^2$$

$$10^5 \times C = 2.38 + 9.59 \times 10^{-3} \times T_{bl} + 9.42 \times 10^{-5} \times T_{bl}^2$$

The approximate equations that presented previously in the above sections are normally developed to predict the simulation of the MSF process and collector performance. Calculations made to determine variations in fluid properties and flow conditions. Material and energy balance equations around the stage are combined and arranged to yield a set of independent simultaneous equations. The previous equations are simultaneously solved by matrix algebra to determine the main unknown performance parameters (T_{bo}, B_l, T_{Fo}, T_{dl}, and DP). Water physical properties are calculated as a function of temperature. Using the real measured data of different physical and operating conditions as input data, the daily productivity of the system is calculated. Using these conditions, with initializing the unknown temperatures; the system units' heat transfer coefficients are calculated too. With a reasonable specific tolerance, the mathematical model is solved by Gauss–Seidel iteration method. The iteration is continued until the following inequality is valid $\left|\frac{T_{calculated} - T_{assumed}}{T_{assumed}}\right| \leqslant 0.001$.

5. Results and comments

For illustration, the detailed results for just two days (one during the summer season and the other during the winter) are considered in the following sections.

5.1. Summer results

The measured data and parameters obtained on 22 June 2005 are illustrated in Tables 2 and 3. The feed water flow rate is considered to be constant and equal to 0.0183 kg/s. During the operating hours, the system goes under steady state conditions. Losses from the flash unit to the ambient are neglected.

The measured data show that the system productivity is 11 kg/day. For 22 June 2005, the average total solar irradiance obtained on the collector surface is about 4.45 kW h/m^2. Fig. 6 shows the hourly variation in solar radiation during 22 June 2005. The mean values of the fractional percentage error between the theoretical and the experimental results are about 2% (see Table A.1). Fig. 7 shows the characteristic efficiency and operating temperatures curves of the solar collector. Efficiency curve is based on gross collector area and is determined using the outdoor conditions. It seen from the thermal efficiency curve that the thermal efficiency of the solar collector is not a constant but a highly variable characteristic depending on the outdoor temperature, the level of solar radiation, and the temperature of the fluid at the inlet. So the instantaneous efficiency is obtained by dividing the energy obtained from the collector over the proper time period by the integrated value of incident solar energy over the period. The thermal efficiency of the collector is presented as follows [11]:

$$\eta_c = F_R(\tau\alpha) - F_R U_l\left(\frac{T_{icol} - T_{amb}}{I_S}\right) \tag{23}$$

It should be noted that the mean plate temperature T_{mp} can be approximately related to the average fluid temperature and that is clearly seen in Fig. 7. Fig. 7 gives a clear view about the collector ranking relative to any other collectors due to the efficiency factor and heat removal factors values.

Figs. 8–10 show the experimental and theoretical results of the system operation during 22 June 2005. Fig. 8 represents the temperature distribution of the system during the day operation. The temperatures increase gradually due to the changing solar intensity along the day operation. Theoretical and experimental results for the temperature distributions are in good agreement as shown in Fig. 8.

The performance of desalination system is a measure of its efficiency for producing water [17]. So; the system performance ratio can be estimated as follows:

$$PR_n = \frac{\sum_{1\ldots n} \dot{D}_{tn} \times Hv_n}{I_S \times A_c} \tag{24}$$

where I_S is the solar intensity in kW/m^2, A_c is the collector heat transfer area in m^2, Hv_n is the latent heat of vaporization at stage (n) and $\dot{D}_{tn}$ is the rate of total productivity at stage (n).

Table 2
Measured weather conditions and results on Julian day 173 in June 2005

	Time (h)								
	–	9	10	11	12	13	14	15	16
I_S (W/m^2)	–	450	562	650	680	648	571	474	415
T_{amb} (°C)	–	26	27	28	29	30	30	31	30
V_w (m/s)	1.3								
T_{Fi} (°C)	27								
T_{Fo} (°C)	–	31	36	38	39	37	36	36	36
TBT (°C)	–	50	52	54	56	52	50	50	49
T_{b1} (°C)	–	37	39	41	42	40	39	39	37
T_{d1} (°C)	–	32	37	39	40	38	37	37	36
T_g (°C)	–	33	33	34	35	34	34	33	33
T_{icol} (°C)	–	31	36	38	39	37	36	36	36
T_{ocol} (°C)	–	50	52	54	56	52	50	60	59
PR (–)	–	0.7	0.85	0.8	0.9	0.8	0.8	0.9	0.9
T_{ins} (°C)	31								
F_S (kg/s)	0.0183								
Product (kg/day)	11								

Table 3
The estimated energy values through the solar collector on Julian day 173 in June 2005

Q_{stg} (W/m^2)	–	0.02	0.62	1.34	1.65	1.39	0.71	0.13	0
Q_{loss} (W/m^2)	–	64.52	78.73	89.55	91.37	80.89	69.86	56.68	50.87
Q_u (W/m^2)	–	385.4	482.6	559.09	587.01	565.7	500.4	417.18	364.22
U_{loss} (W/m^2 K)		3.98	3.91	4.01	4.04	4.05	4.03	4.02	4.02
U_{tloss} (W/m^2 K)	–	2.26	2.31	2.35	2.38	2.39	2.37	2.36	2.36
U_{eloss} (W/m^2 K)	0.309								
U_{bloss} (W/m^2 K)	1.35								
Efficiency factor	0.93								
Heat removal factor	0.88								

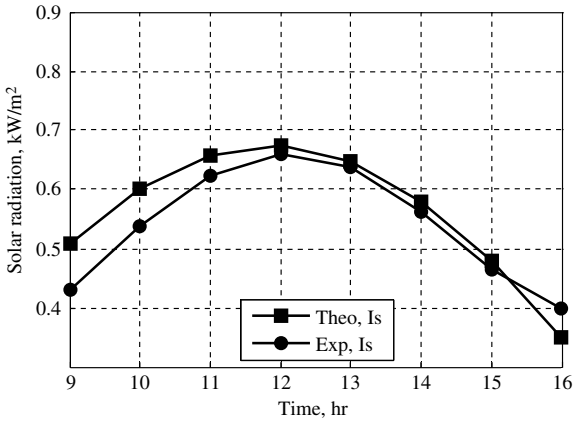

Fig. 6. The hourly variation in solar radiation during the 22nd of June 2005.

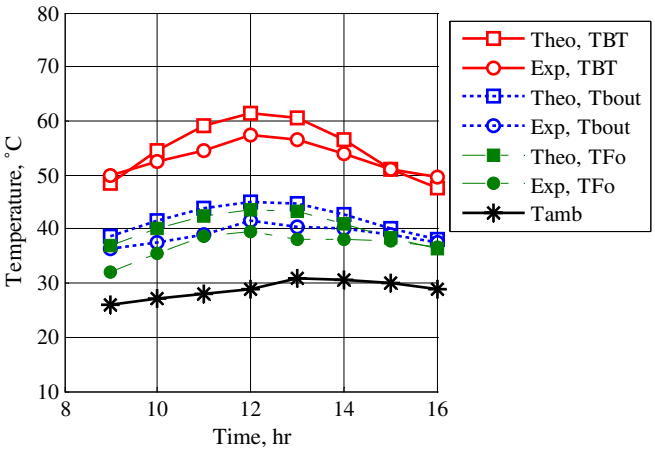

Fig. 8. The temperature distribution of the system along the day operation during the 22nd of June 2005.

The stage temperature drop ΔT_{st} is equal to the difference between TBT and that of the wasted blow down brine T_{b1} and is known as the flashing range. Fig. 9 shows the hourly variations in the system performance ratio (PR) and the flashing range ΔT_{st}. The figure shows that the PR ranges between 0.8 and 0.9 and ΔT_{st} ranges between 11 and 12 °C.

Fig. 10 shows the system hourly productivity on the same day in June. The accumulative productivity on this day is about 4.6 kg/day/m^2.

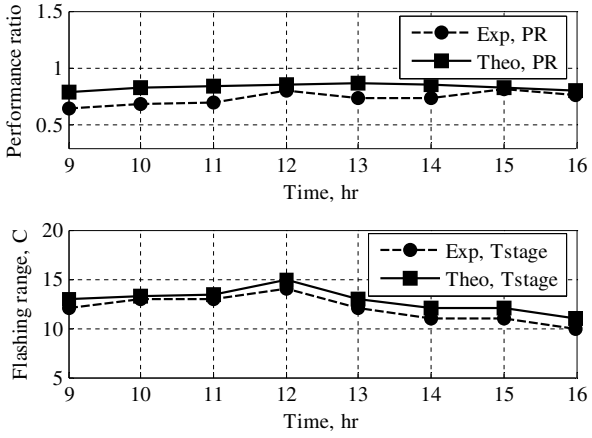

Fig. 9. The system performance ratio and the system flashing range during the 22nd of June 2005.

5.2. Winter results

Table 4 shows the measured data on 21st January 2005 as an example of the winter conditions. The table shows that the productivity is 1.04 kg/day/m^2. The TBT is recorded as 38–42 °C, which is considered too low to drive the flashing operation. The maximum obtainable solar intensity on that day was 447 W/m^2. This value of the measured solar flux is too weak to produce a suitable TBT. Generally, the fresh water productivity and the performance ratio of the system are smaller in winter operation than summer operation.

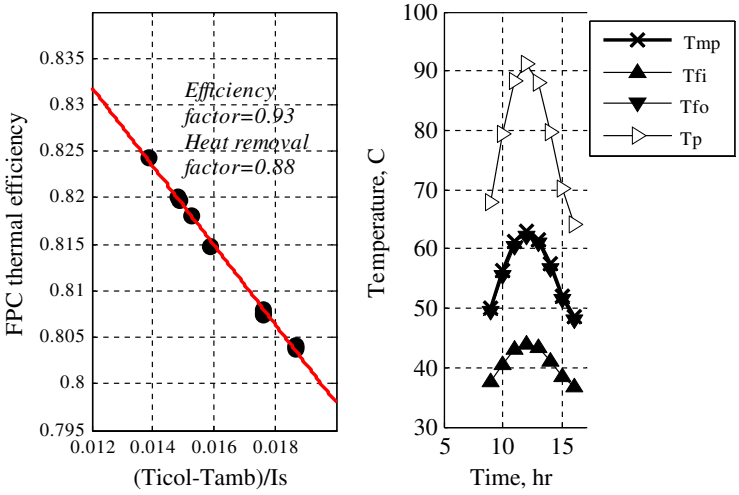

Fig. 7. The characteristic efficiency and operating temperatures curves of the solar collector.

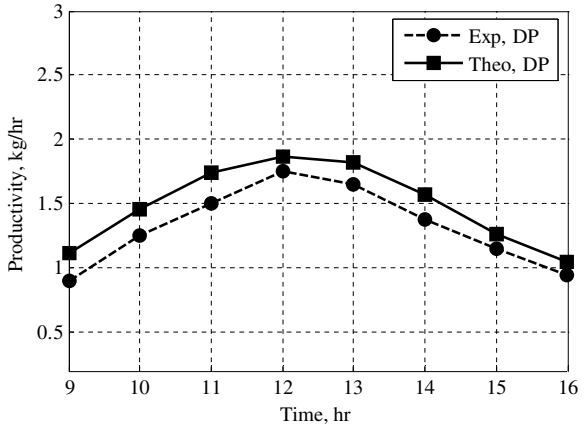

Fig. 10. The hourly productivity of the system during the 22nd of June 2005.

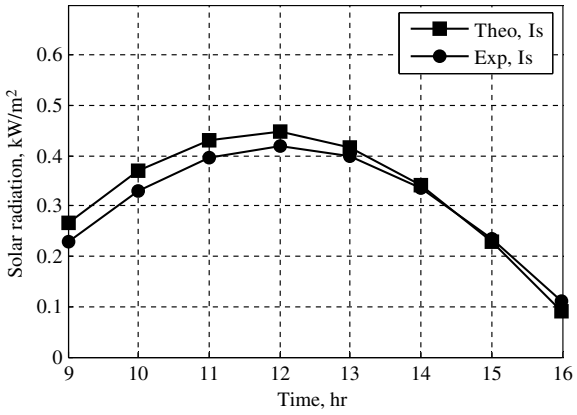

Fig. 11. Variation of solar radiation with time during the 21st of January 2005.

Fig. 11 shows the variations of solar radiation on 21st January 2005. The figure illustrates the agreement between the theoretical model results of solar radiation (BIRD model) and the measured results, indicating that the maximum error is 2%. Fig. 12 shows the system temperature distribution along the day operation hours. It is seen from Fig. 12 that the temperatures are increasing gradually until mid day hour then decreases gradually at the shut off of operation hours. Also, the figure shows a good agreement between the theoretical and experimental results. Fig. 13 shows both the PR and the flashing range ΔT_{stg}. The PR does not exceed about 0.7 to 0.8 in winter, and ΔT_{st} ranges from 10 to 12 °C.

Fig. 14 shows the hourly productivity of the system. The figure shows a comparison and an acceptable difference between the theoretical and measured results with an error about 9%. The total distillate productivity DP does not exceed about 1.04 kg/day/m^2 on 21st January 2005. The lower productivity in winter is caused by the lower solar intensity compared with the summer results.

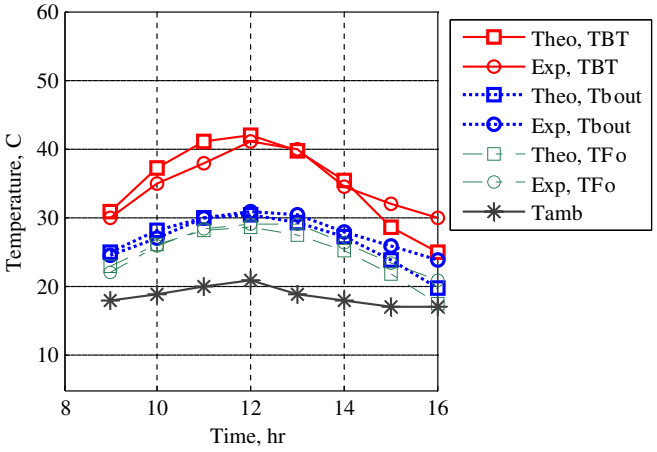

Fig. 12. The temperature distribution of the system during the 21st of January 2005.

Following the same sequence for the days along one year, the average measured data and results are presented in Table 5.

Table 4
Measured weather conditions and results on Julian day 21 in January 2005

	Time (h)								
	9	10	11	12	13	14	15	16	17
I_S (W/m^2)	266	370	432	447	415	341	230	90	–
T_{amb} (°C)	17	18	22	23	22	21	20	19	17
V_w (m/s)	1.5								
T_{Fi} (°C)	18.5								
T_{Fo} (°C)	22	25	27	28.5	26	25.5	23.5	21.5	
TBT (°C)	38	39	40	42	41	41	40	39	–
T_{b1} (°C)	24.5	28	30	32	31	31	30	29	–
T_{d1} (°C)	22	25	27	28	26	25	23.5	21.5	–
T_g (°C)	22	23	25	25	23	23	22	21	–
T_{icol} (°C)	22	25	27	28.5	26	25.5	23.5	21.5	–
T_{ocol} (°C)	38	39	40	42	41	41	40	39	–
PR (–)	0.6	0.65	0.7	0.85	0.8	0.75	0.6	0.6	–
T_{ins} (°C)	21								
F_S (kg/s)	0.0183								
Product (kg/day)	2.5								

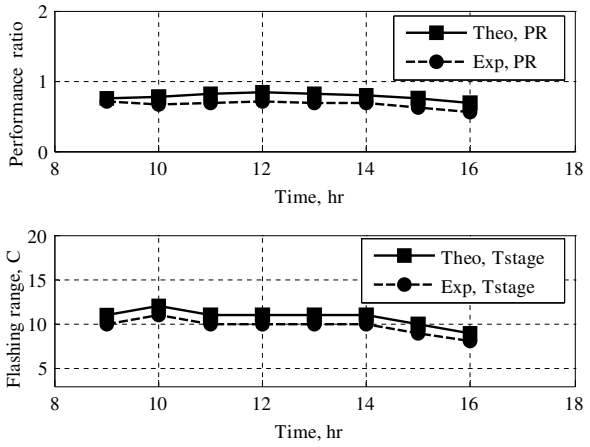

Fig. 13. The system unit performance ratio and the system flashing range during the 21st of January 2005.

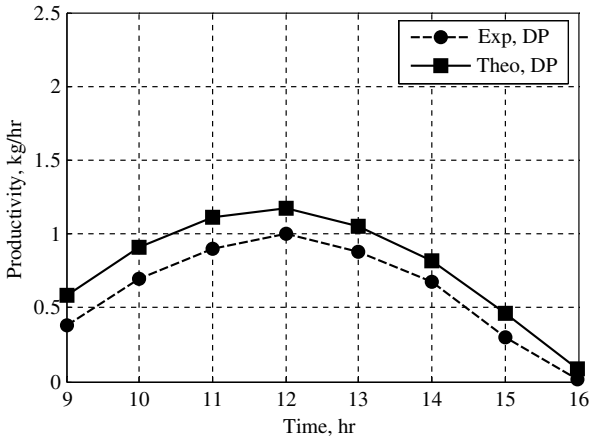

Fig. 14. The hourly productivity of the system during the 21st of January 2005.

Table 5
The average values obtained for the system operation along one year

Month	T_{Fi} (°C)	T_{Fo} (°C)	TBT (°C)	T_{b1} (°C)	I_S (W h/m^2)	T_{amb} (°C)	T_g (°C)	T_{ins} (°C)	V_w (m/s)	Product (kg/day)
1/2005	18	25.125	40	26	3144	20	24	22	2.25	2.5
2/2005	19	25.357	44.25	28	3469	23	30	26	1.3	4.5
3/2005	20.25	28.125	48	34.5	4049	24	30.5	27	4.2	6.5
4/2005	22.6	32	49	35.5	4462	25	31	28.25	3.7	8
5/2005	24	34	52	36.5	4495	27.5	30	30	1.05	8.5
6/2005	27.25	36.125	53	40	4750	29	34	30.25	2.5	11
7/2005	27.6	38	60	44	4867	31	35	32.357	1.5	14
8/2005	28.75	39	67	43.75	5120	33	36.5	34.5	0.8	16.5
9/2004	26.75	36.5	52	42	4601	29	36.5	30.75	3.25	12
10/2004	26.5	35.25	49	37	3858	28	35.6	31	3.7	9
11/2004	20.375	34	44	35	2888	23	32	30	3.8	5
12/2004	17.125	32	42	34.5	2791	19	28.5	23.5	1.625	3.5

6. Conclusion

Solar water desalination system using flashing process is constructed and operated at the Faculty of Petroleum and Mining Engineering at Suez-Egypt. The system consists of a solar water heater (flat plate solar collector) working as a brine heater, and a single vertical flash chamber which is attached with a condenser/preheater unit. The collector surface area is about 2.39 m^2, and condenser surface area is about 1.388 m^2. A mathematical model is developed for the all system components (collector, flash unit, condenser unit) to predict the system productivity under different and wide range of operating conditions. The test rig works better at higher TBT, i.e., higher solar intensity. Reasonable rate of feeding water is ranged about 0.0183 kg/s. The system daily productivity in summer is about 4.2 to 7 kg/day/m^2, and about 1.04 to 1.45 kg/day/m^2 during the winter season. The unit performance ratio is varied between 0.7–0.8 in winter and 0.8–0.9 in summer. These values are typical for a single stage MSF system. The collector efficiency factor is about 0.93 and the heat removal factor is about 0.88. Increasing the solar radiation would increase the system productivity. The results of the proposed mathematical model are in good agreement with those of the experimental model of the system. Producing fresh water by this solar desalination system with its simplicity would be one of the best solutions to supply water for small groups with no technical facilities.

Appendix A

A.1. Error analysis of the experimental work

The measured experimental data includes some errors due to the uncertainty of the measuring process and the limited precision of the experimental instruments. For examination of the validity of the experimental work; the following fractional error (Fr) equation is used:

$$\%\mathrm{Fr} = \frac{\text{Calculated} - \text{Measured}}{\text{Calculated}} \times 100$$

The average Fr percentage for measuring the solar radiation was about 1–2%. For the TBT; the Fr error; did not exceed about 6–7%. Also, for the wasted brine and outlet

Table A.1
The Fr error percentage of measured data

Parameter	Fr percentage (%)
I_S	2
TBT	6–7
T_{b1}	9
T_{icol}	8
DP	7
PR	4

feed water temperatures; the percentages were about 9% and 8%, respectively. The percentage for the system performance ratio PR is about 4% and 7% for the system productivity DP (see Table A.1).

References

[1] El-Dessouky Hisham T, Ettouney Hisham M, Al-Roumi Yousef. Multi-stage flash desalination: present and future outlook. Chem Eng J 1999;73(February):173–90.
[2] Zhang Lianying, Zheng Hongfei, Wu Yuyuan. Experimental study on a horizontal tube falling film evaporation and closed circulation solar desalination system. Renew Energy 2003;28(October):1187–99.
[3] Soliman A. Study of water desalination by solar energy using humidification- dehumidification processes. MSc thesis, Mechanical Engineering Department, Faculty of Petroleum and Mining Engineering, Suez Canal University, Egypt, 2002.
[4] El-Nashar Ali M. The economic feasibility of small solar MED seawater desalination plants for remote arid areas. Desalination 2001;134:173–86.
[5] Garcia-Rodriguez Lourdes, Gomez-Camacho Carlos. Preliminary design and cost analysis of a solar distillation system. Desalination 1999;126:109–14.
[6] Badran OO, Al-Tahaineh HA. The effect of coupling a flat plate collector on the solar still productivity. Desalination 2005;183: 137–42.
[7] Kriesi R. Design and operation experience with solar powered multistage desalination plants. Desalination 1981;39:109–16.
[8] Rajvanshi Anil K. A scheme for large scale desalination of sea water by solar energy. Sol Energy 1980;24:551–60.
[9] Ziad M, Tleimat Badawi W. Test results from a solar boiler for saline water distillation. Desalination 1981;39:63–70.
[10] Bird Richard E, Hulstrom Roland L. A simplified clear sky model for direct and diffuse insolation on horizontal surfaces. Colorado USA: Solar Energy Research Institute, Golden; 1981.
[11] Jansen Ted J. Solar engineering technology. New Jersey, USA: Englewood Cliffs; 1985.
[12] Simon Frederick F. Flat plate solar collector performance evaluation with a solar simulator as a basis for collector selection and performance prediction. Sol Energy 1976;18:451–66.
[13] Duffie JA, Beckman WA. Solar engineering of thermal processes. 2nd ed. New York, USA: John Wiley; 1991.
[14] Nafey AS. Design and simulation of seawater-thermal desalination plants. PhD thesis, Leeds University, 1988.
[15] Al-Ajlan SA, Al Faris H, Khonkar H. A simulation modeling for optimization of flat plate collector design in Riyadh, Saudi Aribia. Renew Energy 2003;28:1325–39.
[16] El-Dessouky Hisham T, Shaban Habib I, Al-Ramadan Hamida. Steady-state analysis of multi-stage flash desalination process. Desalination 1995;103:271–87.
[17] Al-Hengari Salah, El-Bousiffi Mohamed, El-Mudir Walid. Performance analysis of a MSF desalination unit. Desalination 2005;128:73–85.